Carbohydrate Polymers 102 (2014) 55–65

Contents lists available at ScienceDirect

Carbohydrate Polymers

journal homepage: www.elsevier.com/locate/carbpol

Tamarindus indica pectin blend film composition for coating tablets with enhanced adhesive force strength

Rajneet Khurana, Kuldeep Singh, Bharti Sapra, A.K. Tiwary, Vikas Rana*

Pharmaceutics Division, Department of Pharmaceutical Sciences and Drug Research, Punjabi University, Patiala 147002, India

ARTICLE INFO

Article history:
Received 25 July 2013
Received in revised form 4 September 2013
Accepted 4 November 2013
Available online 13 November 2013

Keywords:
Tablet coating material
Tamarind pectin
CH–TP films
Adhesive force strength
Film rolling effect

ABSTRACT

Tablet coating is the most useful method to improve tablet texture, odour and mask taste. Thus, the present investigation was aimed at developing an industrially acceptable aqueous tablet coating material. The physico-chemical, electrical and SEM investigations ensures that blending of *Tamarindus indica* (Linn.) pectin (TP) with chitosan gives water resistant film texture. Therefore, CH–TP (60:40) spray coated tablets were prepared. The evaluation of CH–TP coated tablets showed enhanced adhesive force strength (between tablet surface to coat) and negligible cohesive force strength (between two tablets) both evaluated using texture analyzer. The comparison of CH–TP coated tablets with Eudragit coated tablets further supported superiority of the former material. Thus, the findings pointed towards the potential of CH–TP for use as a tablet coating material in food as well as pharmaceutical industry.

1. Introduction

The industrial demand of putative form of polysaccharides or their synthetic derivatives has been increasing due to their safety, biodegradability, biocompatibility and non-toxicity. This is because they are acceptable as thickening agent, gelling agent, emulsifying agent, binding agent, encapsulating agent, swelling agent, disintegrating agent, foam stabilizer, etc. (Prajapati, Jani, Moradiya, & Randeria, 2013; Rana et al., 2011; Singh, Tiwary, & Rana, 2013a; Singh, Tiwary, & Rana, 2013b). In addition, the chemical modification of these polysaccharides further improves their physico-chemical as well as mechanical properties.

Tablet coating is the most preferred technique to improve tablet texture, mask taste, odour, sustained delivery, enteric delivery and targeted delivery of drug(s). In a traditional aqueous sugar coating process, natural gums are added to improve the texture of the coating surface as well as to enhance the adhesion of the coat with the uncoated tablet surface. However, this type of aqueous coating process needs expert personal due to the drawback of batch to batch variation in appearance as well as in vitro performance. In addition, nonavailability of a simple coating process, increased labour input and availability of cheap synthetic nonaqueous coating process using synthetic nonbiodegradable polymers seems to reduce the performance of aqueous coating process (Rai, Tiwary, & Rana, 2012a). Hence, a need was to provide a natural, biodegradable, industrially acceptable cheap polysaccharide as a coating material and an optimized tablet coating process that could improve the tablet texture, taste and odour. Further, natural or modified polysaccharides such as guar gum, *Cassia fistula* gum, pectin, konjac glucomannan, etc., have been widely investigated for the peroral delivery of drugs and were known to improve tablet texture and to some extent odour of a tablet (Rana et al., 2011; Rai, Tiwary, & Rana, 2012b). However, they did not contribute to improve taste of tablets. Pectin is an edible and water soluble polysaccharide which consist primarily of D-galactouronic acid. These D-galactouronic acid units contain carbonyl groups (COO^-) and some of these carbonyl groups were methoxylated (Chen et al., 2010; Muzzarelli et al., 2012). The variation in the content of methoxylation as well as carboxyl group affects taste behaviour and physicochemical properties of pectin depending upon the source (Caluwe, Halamova, & Damme, 2010; Tripathi, Mehrotra, & Dutta, 2010, Jindal, Kumar, Rana, & Tiwary, 2013a). Among pectin containing fruits, tamarind pectin is available in variable tastes depending upon its D-galactouronic units, methoxylated content and tartaric acid content. They are the fruits of *Tamarindus indica* L. belongs to the sub-family Caesalpinioideae of the family Leguminosae or Fabaceae (Kaur, Yadav, Ahuja, & Dilbaghi, 2012; Kumar & Bhattacharya, 2008). Tamarind fruit is a pulpy mass of a light reddish-brown colour, changing with age to a dark brown, containing some branching fibres and numerous reddish brown, smooth, oblong or quadrangular, compressed seeds, each enclosed in a tough membrane. Tamarind seeds contain tamarind seed polysaccharide (TSP). The TSP was reported to act as binding agent, emulsifier, suspending agent, sustaining the drug release,

* Corresponding author. Tel.: +91 9872023038.
E-mail address: vikas_pbi@rediffmail.com (V. Rana).

0144-8617/$ – see front matter © 2013 Elsevier Ltd. All rights reserved.
http://dx.doi.org/10.1016/j.carbpol.2013.11.005

hydrogels, mucoadhesive agent, rectal drug delivery and nasal drug delivery properties (Prajapati et al., 2013; Rana et al., 2011). In addition, various derivatives of TSP (acetyl, hydroxyalkyl, carboxymethyl, crosslinking using epichlorohydrin, partial degradation of galactosidase, polyelectrolyte complexation, etc.) have been explored in bioadhesive, nasal, sigmoidal, various drug delivery systems (Goyal, Kumar, & Sharma, 2007; Goyal, Kumar, & Sharma, 2008; Kaur, Jain, & Tiwary, 2010; Kaur, Mahajan, & Bassi, 2013; Prajapati et al., 2013). However, tamarind fruit pulp is still considered as a food or some applications in traditional herbal drugs to treat diseases like prevention of cardiovascular diseases by lowering of serum lipids and as antioxidant (50 and 100 mg/kg p.o), immune regulatory effects in the intestine and lowering the postprandial glucose response, as antimicrobial (250 mg/kg) for chronic diarrhoea and dysentery and as an astringent (10 mg/kg) (Al-Fatimi, Wurster, Schröder, & Lindequist, 2007; Caluwe et al., 2010; Jindal, Dhingra, Sharma, Parle, & Harna, 2011; Lim, Mat Junit, Abdulla, & Abdul Aziz, 2013; Nwodo, Obiiyeke, Chigor, & Okoh, 2011; Souza and Aka, 2007). Since they are also dietary fibres, being non-digestible dietary carbohydrates, they also show effects on bowel movement (Muzzarelli et al., 2012). The tamarind fruit pulp contains tamarind pectin (2–4%, w/w). Chemically, tamarind pectin consists of α-(1-4)-D-galacturonic acid units, interrupted by the insertion of rhamnose units and with side chains of neutral sugars (galactose, arabinose and rhamnose) attached to the backbone (Goyal et al., 2007, 2008; Sato, Oliveira, & Cunha, 2008).

Oliveira, Ferrari, Carvalho, and Evangelista (2010) developed chitosan–pectin–calcium multiparticulate systems for colonic drug delivery. A carboxylic group of pectin (low methoxy) was interacted with chitosan to form nanocarriers for sustained and targeted delivery of diclofenac sodium (Dutta & Sahu, 2012). Hence, incorporation of $CaCl_2$ into and CH pectin to prepare CH–Ca–pectin films was found to affect physico-chemical and mechanical properties of films as between CH and pectin. This is because, the presence of other intercations between CH and pectin like hydrogen bonding could not be ruled out. This hydrogen bonding could be hindered in the presence of Ca. Further, it is interesting to note here that chitosan was immediately interacted with pectin to form gelatinous precipitates. These gelatinous precipitates were easily utilized in the fabrication of microspheres, nanocarriers, beads, microgels, crosslinked films, etc. (Jindal, Kumar, Rana, & Tiwary, 2013b; Kaur et al., 2010, 2013; Luppi et al., 2010; Morris, Foster, & Harding, 2000; Morris, Kok, Harding, & Adams, 2010; Puga, Lima, Mano, Concheiro, & Alvarez-Lorenzo, 2013). However, these gelatinous precipitates of interaction between chitosan and pectin were either unable to spray dry or to formulate into films. Hiorth, Tho, and Sande (2003) sprayed both pectin solution and chitosan solution separately but simultaneously sprayed through two nozzles to obtain CH–pectin films. Therefore, CH carbamate salt in alkaline medium was prepared to obtain clear solution with polyanion (Muzzarelli, Stani, Gobbi, Tosi, & Muzzarelli, 2004; Muzzarelli and Muzzarelli (2005)) or ammonium acetate was added to slowdown the reaction between chitosan and pectin (Singh, Suri, Tiwary, & Rana, 2012) or sometime a combination of $CaCl_2$ with pectin to control the reaction with chitosan was employed (Lootens et al., 2003). Therefore, an attempt was made to identify polyanionic pectin that forms a clear solution in acetic acid solution of chitosan. This could avoid the formation of chitosan carbamate, addition of ammonium acetate/$CaCl_2$ step necessary for the formation of uniform chitosan–pectin films. Tamarind pectin (TP) is acidic in nature (Caluwe et al., 2010; Yapo, 2011). This acidic nature of TP was due to increased —COOH group present in it instead of $—COO^-$ groups. Thus, it is expected to form a clear solution with cationic chitosan (positively charged) in acetic acid solution. This clear solution could be easily sprayed to form and generate sweet taste tablet coating material along with improved tablet texture and odour.

Therefore, the aim of the present study was to examine possibilities of tamarind pectin as a tablet coating material. This aim was fulfilled by preparing chitosan–tamarind pectin blend films without using reaction controllent and evaluate the changes in physicochemical, electrical, mechanical properties as well as coat strength behaviour to explore their potential in pharmaceutical industry.

2. Materials and methods

2.1. Materials

Tamarind fruits were procured from local market (Patiala, India). Mesalamine (taken as model drug) procured from Sun Pharmaceutical Industries Ltd. (India). Chitosan (85% deacetylated) was obtained from Indian Sea Foods, Cochin (India). Acetone AR was procured from Loba Chemie Pvt. Ltd. (Mumbai, India). All other chemicals used were of analytical grade and used as received.

2.2. Extraction of tamarind pectin (TP)

The extraction procedure adopted for the extraction of TP was modified from the method reported by Kulkarni et al. (2001). The outer epicarp of the fruit was removed gently, the pulp containing seed was soaked in 250 mL of distilled water (pH 5 adjusted with 0.1 N HCl) and was kept for 3–4 h at 45 °C. The seeds were removed from the prepared pulp suspension. The suspension was left overnight in a refrigerator to separate potassium bitartrate. The yellowish powder settled at the bottom of the container was separated from the mother liquor. This pulp suspension was filtered again through muslin cloth to remove any debris. The gelatinous precipitates of TP were obtained when acetone was added into pulp suspension drop by drop. The precipitates were washed with fresh acetone and these precipitates dried in air for 1 h. This pectin was impure. It was again dissolved in water, filtered (G3 filter) and freeze dried. The powder obtained was stored in air tight container in deep freezer till further use. The purity of TP was assured by employing ATR-FTIR and DSC methods. The methoxyl content, glacturonic acid content and degree of esterification of pure TP was found to be $7.12 \pm 0.52\%$, $45.62 \pm 0.975\%$ and $20 \pm 1.89\%$, respectively. The values were in consonance with that reported by El-Siddig et al. (2006) and Itoh et al. (2008) for TP.

2.3. Preparation of CH–TP solution

The total polymer content was fixed to 2%, w/v. For the preparation of CH–TP films, 20–80%, w/v CH was dissolved in glacial acetic acid (3%, w/v) in 25 mL of water. Separately, 80–20%, w/v TP was dissolved in 25 mL of water. After 2 h of stabilization, TP solution was added dropwise to CH solution with constant stirring. A clear homogeneous solution obtained was used for preparing CH–TP films.

2.4. Preparation of CH–TP blend films

Different combination of films containing CH and TP were prepared by spray drying technique. The CH–TP solution was sprayed by employing spray gun (5 mL/min) with the help of peristaltic pump using a spray gun of 1 mm nozzle (Electrolab, PP201V, Mumbai, India) on non-sticky surface of rotating drum with hot air blown at 50 °C for solvent evaporation. The dried films were collected and these films were transferred to microwave (85 W, 15 s, 5 cycles) to remove bound water. The films were stored in large size sealed packs until further use.

2.5. Physical characterization of CH–TP films

2.5.1. Film surface contact angle with pH 1.2, 7.4 or 6.8 buffer

Film surface contact angle with different solvents (pH 1.2, 7.4 or 6.8 buffer) was estimated by obtaining images of a drop of the respective solvent when placed gently over a surface of CH–TP films by employing digital camera (SONY, 14.1 mega pixel, 10× zoom, in mega mode). The contact angle of between drop of the solvent and CH–TP film surface was calculated using software (MB-ruler 3.5). The results reported were mean of 12 determinations (Grzegorzewski, Sascha, Kroh, Geyer, & Schluter, 2010; Singh et al., 2012).

2.5.2. Work of adhesion (W_a)

W_a was calculated from contact angle using the equation:

$$W_a = \gamma_L(\cos\theta + 1)$$

where γ_L is the surface tension of the respective buffer (pH 1.2, 7.4 or 6.8) calculated using stalagamometer method.

2.5.3. Spreading coefficient (S)

S at the buffer film surface was calculated using the equation:

$$S = \gamma_L(\cos\theta - 1)$$

where γ_L is the surface tension of the respective buffer (pH 1.2, 7.4 or 6.8) calculated using stalgamometer method.

2.5.4. Swelling index (SI) of edge sealed CH–TP films

The swelling index of the Eudragit L-100 edge sealed CH–TP films after exposure to different pH was determined by immersing the films in pH 1.2. The swelling index was calculated according to the formula:

$$SI = \frac{W_1 - W_2}{W_1}$$

where W_1 is the initial weight of the film and W_2 is the weight of the swollen film.

For preventing transportation of pH 1.2 buffer through edges of films that causes rolling effect, a pH 1.2 buffer resistant polymer Eudragit L-100 (4%, w/v solution in ethanol) was used to seal edges of CH–TP films.

2.6. Chemical characterization of CH–TP films

2.6.1. FTIR-ATR analysis

A pure sample of CH, TP powder, different CH–TP films were subjected to FTIR-ATR analysis (RXI-JR, Alpha-E, Bruker, Germany) in the spectral region of 500–4000 cm^{-1}.

2.6.2. DSC analysis

CH, TP and CH–TP films were stored in desiccator at 50% RH for 48 h. These samples were subjected to DSC analysis (40–400 °C) employing heating rate of 10 °C/min (Mettler Tolelo Star System, Switzerland).

2.7. Electrical properties of CH–TP films

The electrical behaviour of the film surface was examined by estimating zeta potential of films employing Delsa Nano, Beckman Coulter, USA. Zeta potential was estimated using electrophoretic light scattering method. For this purpose, all the films of 1 × 1 size were fitted over the standard cell (glass). Polystyrene latex solution was used in the standard cell assembly. Light source was laser diode of energy 30 mV with high performance photo-multiplier tube as detector. The zeta potential was obtained and the values reported were mean ± SD of 3 individual determinations.

2.8. Mechanical properties

Mechanical properties (tensile strength and extensibility) of CH–TP films were studied using texture analyzer (Stable microsystem, Godalming, UK) in order to ensure optimum proportion of CH–TP that could achieve maximum interaction density and have sufficient tensile strength. Preliminary settings of texture analyzer for tensile strength estimation were: test mode: tension, pre-test speed – 0.2 mm/s, test speed – 0.5 mm/s, post-test speed – 5.0 mm/s, trigger type – auto, trigger force – 2.0 g, break sensitivity – 5.0 g, probe – A/TG; tensile grips. The films were cut into strip of constant specific length and width. The end of the films was attached to the tensile grips so that the films were neither too tight nor too loose. The test begins with the probe moving at the pre-test speed. The probe pulls the film sample with the test speed. When the elastic limit was exceeded, the film snaps (observed as the maximum tension force).

2.9. Aqueous tablet coating using CH–TP

2.9.1. Preparation of core tablets

The tablets containing mesalamine (MA) as model drug were prepared by employing wet granulation method. Chitosan (3%, w/v) was used as binder (Singh et al., 2012) and prepared in glacial acetic acid (3%, v/v). The tablet blend was prepared by mixing MA (35 mg/tablet) and spray dried lactose (SDL; qs) to 40 mg/tablet. The wet mass was prepared by using chitosan solution (3%, w/v, in glacial acetic acid). The granules were dried at 50 °C for 1 h and regranulated by passing again through #22 sieve and retaining on #44 sieve. The dried granules and colloidal silica (1%, w/w, as glidant) were mixed by tumbling method and compressed using convex six punches, single station rotator compression machine (A.K. Industries, M207, Nakodar, India). The weight of the tablet was 40 ± 0.1 mg and the diameter of the tablet was 4 ± 0.1 mm.

2.9.2. Preparation of CH–TP coated tablets

The CH–TP solution was prepared to coat MA core tablets containing 35 mg MA (as model drug). For preparing CH–TP solution, total CH and TP content was fixed to 1%, w/v. CH (60–80 parts) was dissolved in 50 mL of glacial acetic acid (3%, v/v) solution. Separately, TP (20–40 parts) was dissolved in 50 mL of water and added dropwise to CH solution. The clear solution so obtained was used for coating.

2.9.3. Spray coating of core tablets

For spray coating, core tablets (100 g) were transferred to coating pan. The peristaltic pump (0.1 mL/min) with spray nozzle (1 mm diameter) was used to spray the CH–TP coating solution. The compressed air was introduced at a pressure of 1.5 kg/cm^2. The inlet air temperature was maintained at 60 °C. An increment of 5 mL coating solution was sprayed at each time over the tablet bed in a rotating coating pan with the help of spray nozzle. The tablets were dried and again 5 mL of coating solution was sprayed. The process was repeated until required weight gain of 15%, w/w (approx.) was achieved.

2.9.4. Optimization of tablet coating strength employing texture analyzer

Tablet coating process was optimized using texture analyzer as per method reported by Rai et al. (2012a). Tablet coating strength was estimated by employing texture analyzer (TAXT plus, Stable Microsystems, UK) using tablet-coating strength probe attachment. For the optimization, adhesive force strength and cohesive force strength was determined. For the estimation of adhesive force, a

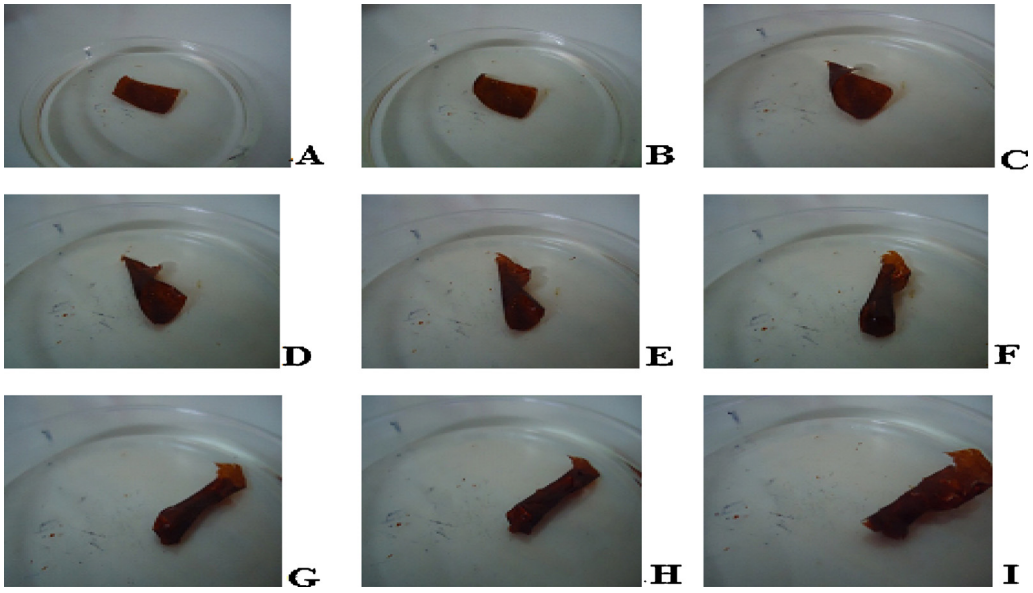

Fig. 1. Rolling effect of pH 1.2, 7.4 and 6.8 on CH–TP films.

coated tablet was fixed at the lower station with the help of double adhesive tape whereas, the upper station containing double adhesive tape only. However, for the estimation of cohesive force, CH–TP films were fixed at the upper station with the help of double adhesive tape. The parameters set for the analysis were: pre-test speed, 1 mm/s; test speed, 0.50 mm/s; post-test speed, 10 mm/s; applied force, 800 g; return distance, 10 mm; and contact time, 10–60 s.

2.10. Surface morphology of tablet coat of CH–TP coated tablets

Scanning electron microscopy (SEM) was used to characterize the effect of different pH (pH 1.2, 7.4 and 6.8 buffer) conditions on the morphology and transverse section of CH–TP tablet coat. The samples were exposed to different pH conditions and subsequently freeze dried. Scanning electron micrograph of surface and transverse section of CH–TP film coats were taken using a SEM (268D, Fei-Philips Morgagni). The samples were coated with gold and mounted in a sample holder. The photomicrographs of sample were taken at an accelerating voltage at 15 kV at different magnifications.

2.11. In vitro drug release behaviour

The mesalamine release from CH-TP coated and core tablet was carried out using USP XXX-NFXXV (Apparatus 1 – Basket method) at 50 rpm and 37 ± 0.5 °C. A 500 mL of 0.1 N HCl was used as a dissolution medium and drug release was studies for 4 h. Aliquots of 5 mL of the dissolution medium was withdrawn after 0.5, 1, 1.5, 2, 2.5, 3, 3.5, 4 h. The volume withdrawn was replaced with fresh dissolution medium. The amount of drug released was analyzed using double beam UV spectrophotometer (Beckman DU-640 B UV/Vis. spectrophotometer) at 300 nm after appropriate dilutions. Each experiment was performed in triplicate.

Further, dissolution data was compared using similarity factor (f_2) and difference factor (f_1) approach. Similarity factor is the logarithmic reciprocal square root transformation of one plus the mean squared (the average sum of squares) differences of drug percent dissolved between the test and the reference products. Difference factor measures the percent error between two curves over all time points (Rai et al., 2012b; Singh, Kumar, Langyan, & Ahuja, 2009). Following equations were used to compare the dissolution behaviour.

$$f_2 = 50 \times \log\left\{\left\{\left[1 + (1/n)\sum_{j=1}^{n}\left|R_j - T_j\right|^2\right]^{-0.5} \times 100\right\}\right\}$$

$$f_1 = \frac{\sum_{j=1}^{n}\left|R_j - T_j\right|}{\sum_{j=1}^{n} R_j} \times 100$$

3. Results and discussion

3.1. Preparation of chitosan–tamarind pectin (CH–TP) films

TP is found to be acidic in nature. Hence, mixing tamarind solution with acidic solution of chitosan did not show any significant change in solution clarity or precipitates, as observed generally in a reaction between anionic polysaccharides (sodium alginate, sodium CMC, etc.) and chitosan solution (in 3%, w/v acetic acid). However, pectins were reported to form hydrogen bonding in acidic environment (Sato et al., 2008). Therefore, a clear solution was poured/sprayed over a smooth hot surface along with hot air drying. Films containing various proportions of CH:TP were prepared and screened on the basis of appearance (Table 1). The results suggested films F1, F2 containing CH:TP in the ratio of 20:80 and 30:70 did not show any film forming properties. The film F3 containing CH:TP in the proportion of 40:60 was brittle. Hence, CH–TP films F4,

Table 1
Results of appearance of films prepared with different proportion of CH:TP.

Ratio of CH–TP	Film code	Appearance	Thickness (mm)
Uniform drying technique			
20:80	F1	Non-uniform	–
30:70	F2	Non-uniform	–
40:60	F3	Brittle	0.149 ± 0.001
50:50	F4	Smooth, flexible film	0.164 ± 0.003
60:40	F5	Smooth, flexible film	0.153 ± 0.001
70:30	F6	Smooth, flexible film	0.155 ± 0.001

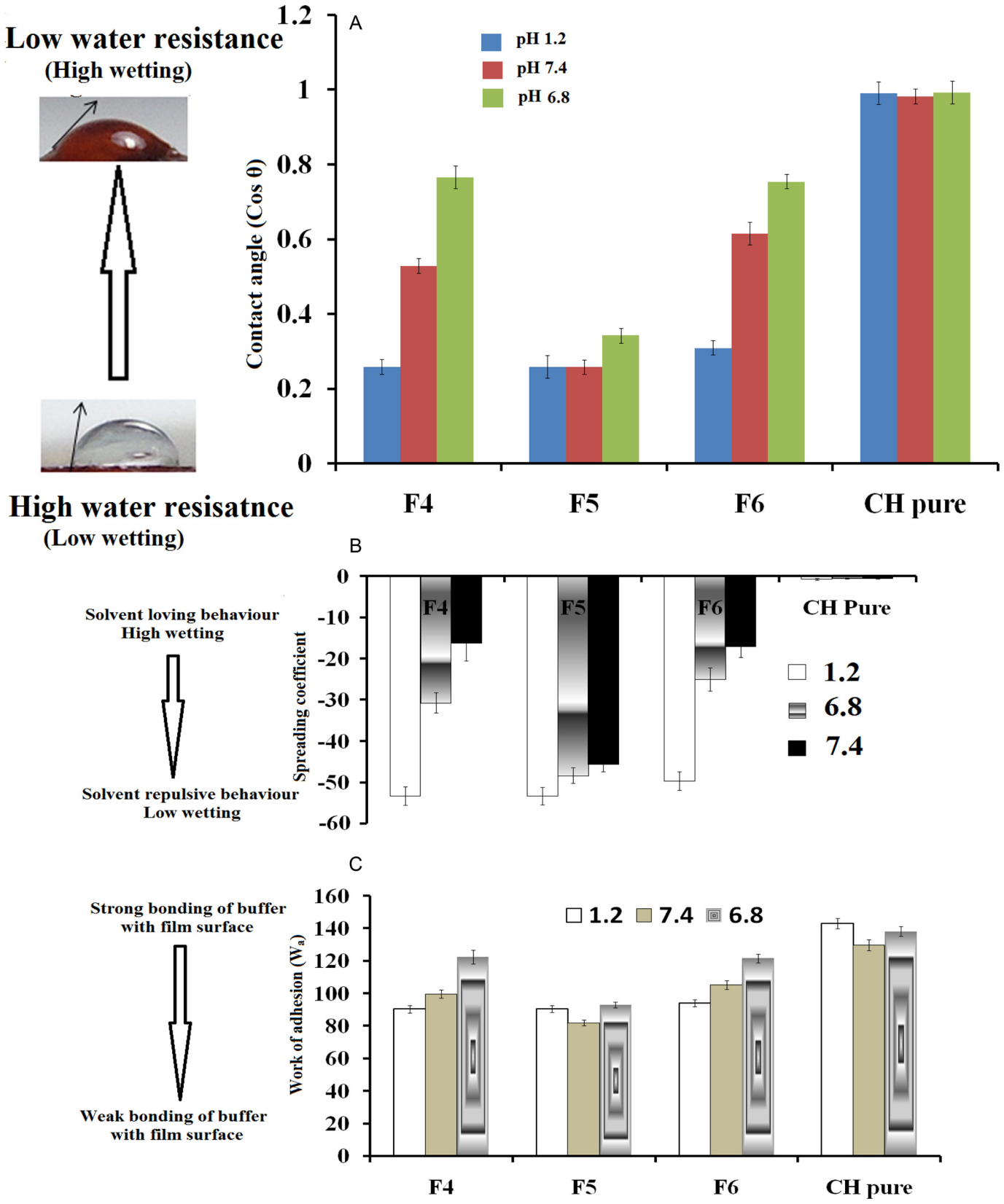

Fig. 2. Influence of different CH–TP films on (A) contact angle, (B) spreading coefficient and (C) work of adhesion.

F5 and F6 could be used for further evaluation as they are smooth and flexible.

3.2. Paradoxical influence of pH on CH–TP films

The CH–TP films containing different proportions of CH to TP were investigated for their response when kept in aqueous environment having pH 1.2, 6.8 and 7.4. When CH–TP films (F4, F5 and F6) were dipped in acidic buffer of pH 1.2, each film starts on rolling from outside to inside to form a tube like structure within a few seconds (Fig. 1). However, when CH–TP films (F4, F5 and F6) were dipped in 6.8 or 7.4 buffer did not show this rolling behaviour as observed in pH 1.2.

3.3. Exploiting the mechanism behind rolling effect

3.3.1. Film surface characterization

The contact angle, work of adhesion and spreading coefficient are the possible tools to explore the reactions occur at the film surface that probably leads to rolling effect. Therefore, contact angle, work of adhesion and spreading coefficients of the solvents; pH 1.2, 7.4 or 6.8 buffer when comes in contact with film surface were employed to envisage the surface nature (water resistance behaviour) of films. The results are summarized in Fig. 2 for pH 1.2, 7.4 and 6.8 buffer. It is well known that water contact angle will increase with increasing water resistance. The value of contact angle ($\cos\theta$) near to one is the indicator of high wetting property. The higher is the work of adhesion, stronger is the bond between buffer and film surface.

The CH acetate films were water soluble and therefore have poor water resistance. Thus, CH pure films were taken as a control to study the film surface behaviour of CH–TP films. The contact angle ($\cos\theta$) of acidic pH 1.2 buffer with CH–TP film surface was found to be less than 0.3 irrespective of the composition of films (Fig. 2A). However, the contact angle ($\cos\theta$) of pH 7.4 or 6.8 buffer with CH–TP and CH pure film surface was found to be more than 0.5, except F6 film. This indicated CH–TP films provide high water resistant surface to acidic pH. Thus, it could be envisaged that contact angle is inversely proportional to interaction potential i.e. higher is the interaction potential, lower is the contact angle ($\cos\theta$). Further, the maximum negative spreading coefficient and minimum work of adhesion of F5 film pointed towards buffer repelling behaviour of CH–TP F5 film surface (Fig. 2B and C).

Hence, the estimation of contact angle between film surfaces to pH 1.2 buffer showed higher water resistance nature as compared to contact angle between film surface to pH 7.4 or pH 6.8 buffer. This suggested inability of pH 1.2 buffer to penetrate inside the CH–TP film. The only possibility of pH 1.2 buffer to enter into the film was from the edges.

Additional films with variable thickness were prepared. Films (F5; 60:40) with four thicknesses 0.156 ± 0.001 mm (F5A), 0.232 ± 0.002 mm (F5B), 0.291 ± 0.001 mm (F5C) and 0.332 ± 0.001 mm (F5D) were prepared. The results suggested only films F5A and F5B showed rolling effect. However, the ability of rolling in presence of pH 1.2 has been lost when thickness was increased above 0.232 mm i.e. films F5C and F5D. Hence, it could be envisaged that penetration of solvent through edges causes rolling effect.

Further, the films F5A, F5B, F5C and F5D were sealed from the edges with the application of alcoholic solution of Eudragit L-100 (a pH 1.2 resistant polymethacrylate derivative) in order to block the movement of solvent through edges. The swelling index of F5A, F5B, F5C and F5D films was found to be negligible. However, the swelling index of control films, i.e. without sealed F5A, F5B, F5C and F5D films was determined to be 0.042 ± 0.011, 0.091 ± 0.010, 0.247 ± 0.011 and 0.473 ± 0.063, respectively. Thus, the findings indicated the difference in rate of penetration of solvent inside the films causes difference in swelling in different parts of films. This probably enhanced protonation of —OH moieties that leads to generation of force for the edge to rolling of the film, since the direct penetration of pH 1.2 buffer was not possible across smooth surface of the film. However, the lower contact angle (higher $\cos\theta$) of pH 7.4 or 6.8 buffer allowed more uniform penetration of pH 6.8 and 7.4 buffer over the film surface. This possibly causes uniform

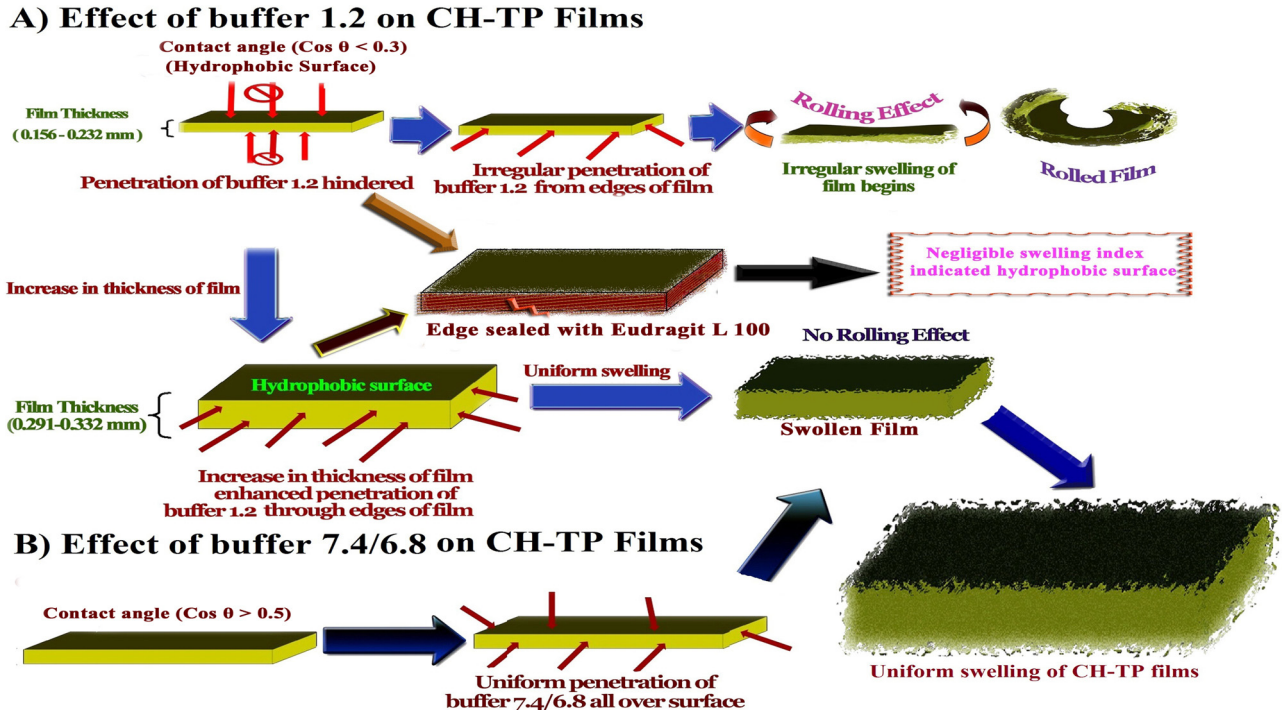

Fig. 3. Exploring the causes of rolling effect in (A) pH 1.2 buffer and (B) pH 7.4 buffer and pH 6.8 buffer.

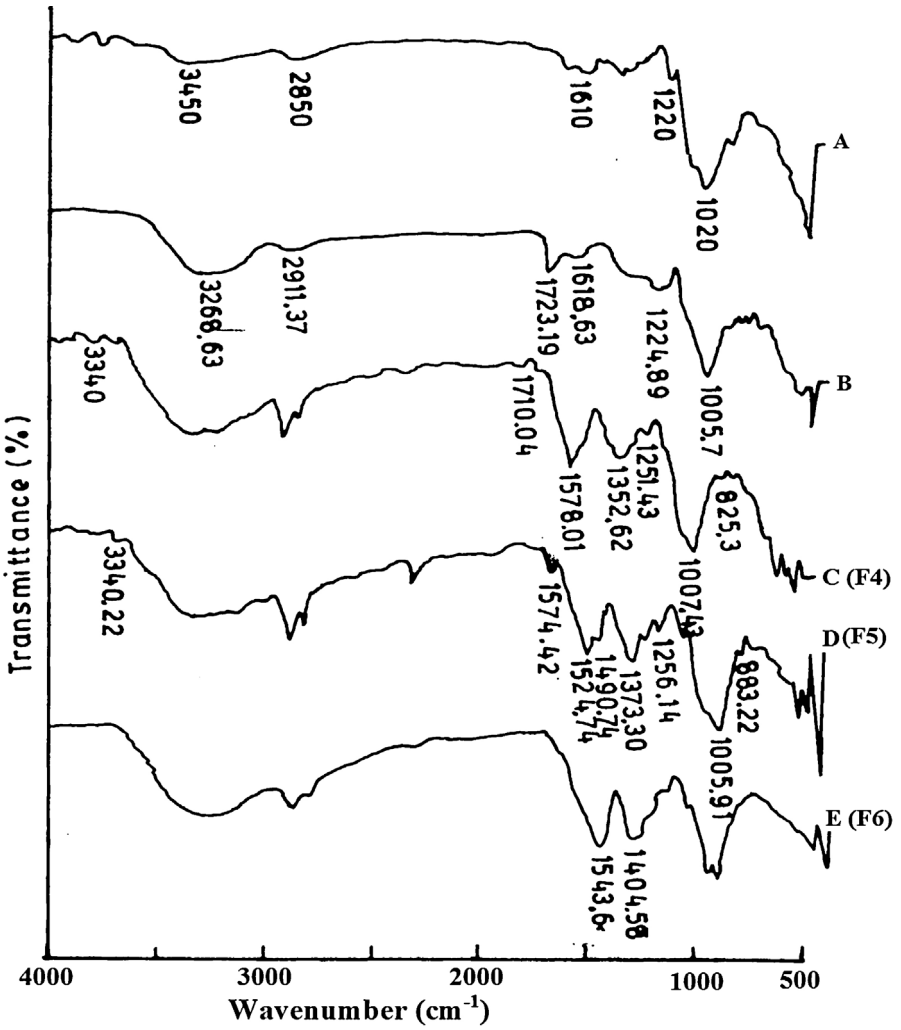

Fig. 4. ATR-FTIR spectra of (A) pure chitosan powder, (B) pure tamarind pectin; CH–TP films formed by co-processing CH and TP in the ratio of 50:50 (F4); (H) 60:40 (F5); and (I) 70:30 (F6).

swelling of film in this environment. A possible mechanism behind rolling effect in pH 1.2 buffer is summarized in Fig. 3.

3.4. Spectral attributes

3.4.1. FTIR-ATR analysis

FTIR-ATR spectra of pure and dried sample of CH (Fig. 4A) showed a broad —OH stretching absorption band between 3450 cm^{-1} and 3100 cm^{-1} and the —CH stretching between 2990 cm^{-1} and 2850 cm^{-1}. Another major absorption band between 1220 cm^{-1} and 1020 cm^{-1} representing the free amino group (—NH_2) at C-2 of glucosamine, a major group present in chitosan. Peak at 1610 cm^{-1} representing acetylated amino group of chitosan, indicated that the sample was not fully deacetylated. The FTIR-ATR analysis of the pure and dried sample of TP exhibited peaks at 3268.63 cm^{-1}, 2911.37 cm^{-1}, 1723.19 cm^{-1} and 1005.7 cm^{-1} corresponding respectively to —OH, —CH, —C=O of ester and acid and —COC stretching of galactouronic acid (Fig. 4B). There was additional strong peaks at 1224.89 cm^{-1} and weak peak at 1618.63 cm^{-1} indicating undissociated carbonyl moieties. However, the peaks exhibiting anionic carboxylic acid characteristic of strong intensity bonds between 1610 cm^{-1} and 1550 cm^{-1} of asymmetrical stretching and 1410 cm^{-1} and 1300 cm^{-1} of symmetrical stretching vibrations of carboxylate group were absent. The dried film F4 showed peaks at 1578.01 cm^{-1}, 1352.62 cm^{-1} and 1251.43 cm^{-1} indicating the presence of anionic carboxylic acid. The peak at 1710.04 cm^{-1} of NH_4^+ moieties of CH suggested the possibility of ionic interaction between the CH and TP (Fig. 4A and C). The additional peaks at 3343.02 cm^{-1} and appearance of strong peak at 1007.43 cm^{-1} followed by a peak at 825.3 cm^{-1} suggested the hydrogen bond formation between the —OH moieties of CH or/and —OH moieties of TP either among themselves or with each other. The FTIR-ATR spectra of spray dried film F5 indicated sharp peaks at 3340.22 cm^{-1} (H-bonding), 1574.42 cm^{-1} (ammonium ion), 1524.72 cm^{-1}, 1490.74 cm^{-1} (asymmetric stretching), 1373.30 cm^{-1}, 1256.14 cm^{-1} (symmetric stretching), 1005.91 cm^{-1} and 883.22 cm^{-1} (hydrogen bonding) suggesting enhancement in interaction density between CH and pectin (Fig. 4D). However, the F6 film exhibited peaks at 1543.61 cm^{-1}, 1404.58 cm^{-1} of antisymmetric and symmetric stretching and absence of peaks in the region 1700–1600 cm^{-1} of ammonium ions suggesting weakening of linkages between CH and TP (Fig. 4E). Further, CH–TP F5 film was found to contains maximum interaction density due to presence of strong H-bonding and carboxylic linkages.

3.4.2. DSC analysis

DSC thermograms of pure CH showed endothermic transitions below 100 °C and one exothermic transition at 311.30 °C. The endothermic transition could be ascribed to the presence of

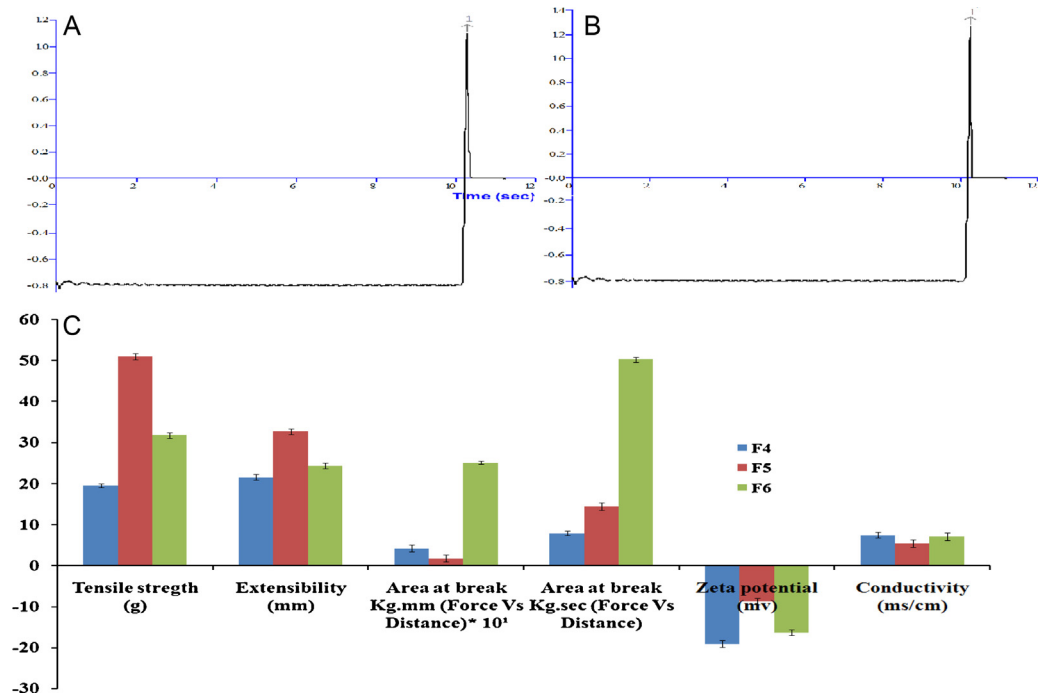

Fig. 5. Mechanical characterization of CH–TP films using texture analyzer: (A and B) typical graph obtained for tensile strength and extensibility of CH:TP films; (C) influence of different CH–TP films on tensile strength, extensibility, zeta potential and conductivity.

moisture or due to the presence of acetic acid moieties (as CH used was 85% deacetylated). The exothermic transition at 311.30 °C could be due to the degradation of CH at this temperature (Table 2). The pure TP showed one endothermic transition at 142.15 °C and one exothermic transition at 291.22 °C. The first endothermic transition could be depicted due to the presence of moisture and hydrogen bonding among the O^- moieties and H^+ moieties of galacturonic acid units (Hiorth, Kjoniksen, Knudsen, Sande, & Nystrom, 2005). The exothermic transition at 291.22 °C could be due to the degradation of pectin at this temperature. A similar peak was observed by Einhorn-Stoll and Kunzek (2009) for DSC behaviour of CH and pure citrus derived pectin.

The DSC thermograms of CH–TP films (F4–F6) showed two endothermic transitions. The first endothermic transition appeared at 104.13–114 °C in almost all the thermograms could be ascribed to be the presence of moisture and/or H-bonding in the films. The second endothermic transition at 220.95–208 °C could be attributed to the carboxylic linkage between COO^- moieties of galacturonic units of TP and NH_4^+ moieties of CH (Rana et al., 2011). The enthalpy (ΔH) of first and second endothermic transition follows the order F5 > F4 > F6. This indicated H-bonding as well as carboxylic linkages were found to be maximum in F5 film. Thus, suggested high level of interaction density that could arises due to presence of both H-bonding and carboxylic linkages.

Table 2
Thermal changes and tablet coating strength of coated tablets when coated with different CH:TP proportions.

Sample	Endotherms				Exotherms	
	First endotherm		Second endotherm		First exotherm	
	T_m (°C)	ΔH (J g^{-1})	T_m (°C)	ΔH (J g^{-1})	T_m (°C)	ΔH (J g^{-1})
CH powder	70.22	−246.00	–	–	311.30	116.46
TP	142.15	−12.84	–	–	219.22	4.143
F_4	104.13	−74.44	220.95	−3.32	–	–
F_5	106.47	−77.80	219.10	−5.67	–	–
F_6	113.98	−31.64	210.10	−13.39	–	–

Tablet coating strength of coated tablets when coated with different CH:TP proportions

Batch no.	Composition of coating solution	Coating surface	Adhesive force strength (g) at contact time (s) of			Cohesive force strength (g) at contact time (s) of		
	CH:TP		10	25	60	10	25	60
T1	50:50	Smooth and uniform	660 ± 2.3	664 ± 1.8	668 ± 1.6	0.82 ± 0.04	0.88 ± 0.05	0.84 ± 0.03
T2	60:40	Smooth and uniform	869 ± 3.2	872 ± 2.9	879 ± 2.3	0	0	0
T3	70:30	Smooth and uniform	597 ± 2.1	600 ± 2.7	610 ± 2.2	0.08 ± 0.005	0.07 ± 0.006	0.07 ± 0.003
Control								
Control TE	Eudragit L 100 (1%, w/v) in alcohol	Smooth and uniform	790 ± 2.5	723 ± 2.7	795 ± 2.3	0.01 ± 0.001	0	0

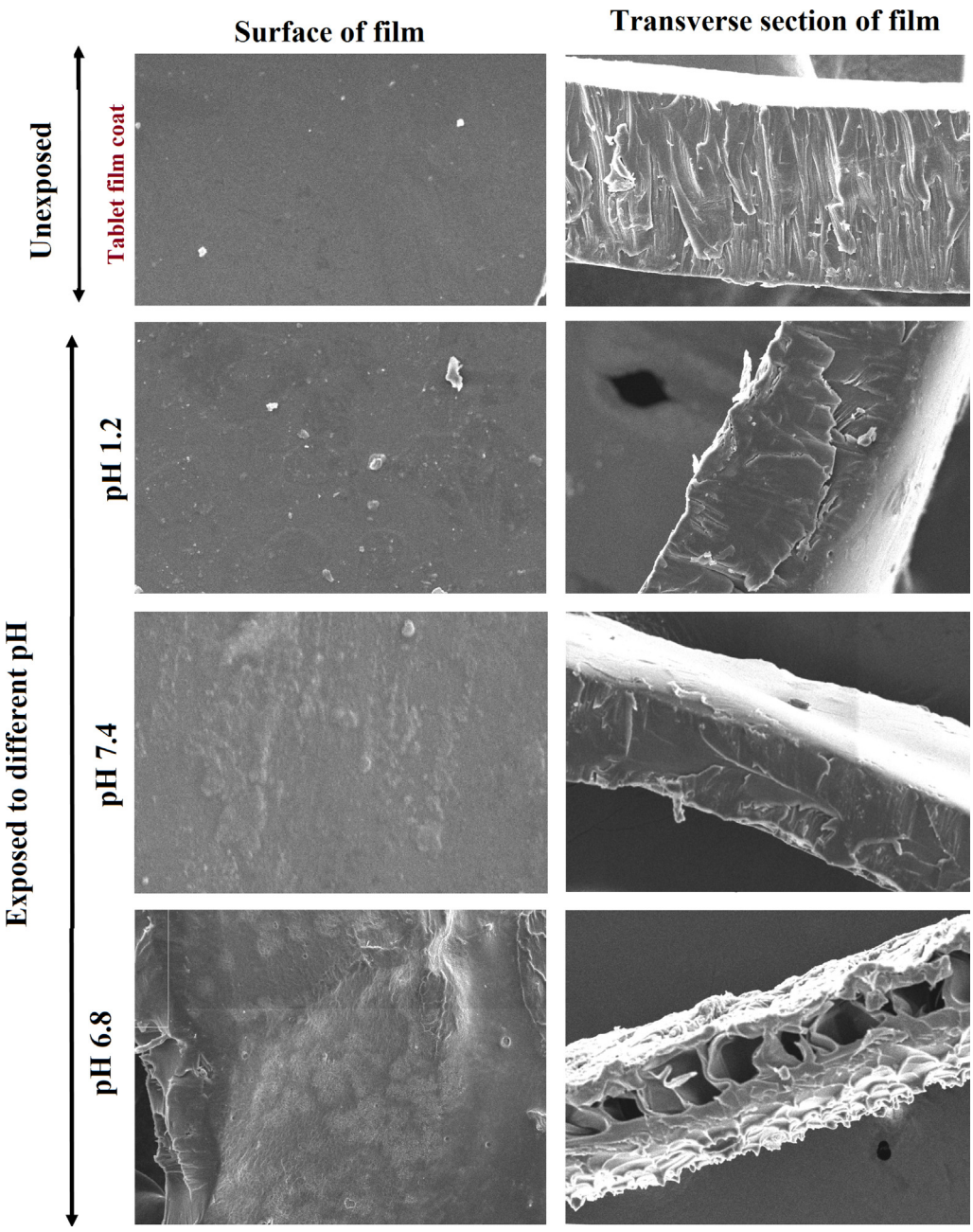

Fig. 6. Surface morphology and transverse section of CH–TP fresh films and films exposed to pH 1.2, 7.4 and 6.8.

3.5. Mechanical characterization using texture analyzer

The mechanical properties of films studied to evaluate the tensile strength and extensibility. Tensile strength is an indicator of toughness of a film. Fig. 5A and B shows typical graphs obtained for tensile strength and extensibility. The results of tensile strength and extensibility of CH–TP are depicted in Fig. 5C. The results suggested enhancement of tensile strength with increase in proportion of CH in film. Interestingly, the extensibility was found to increase with increase in concentrations of CH and decrease in proportion of TP suggesting CH enhanced extensibility of films. Similarly, the area of force vs. time plot and force vs. distance plot was found to enhance with increase in proportions of CH. This was probably due to the enhancement of extensibility of films with decrease in proportion of TP. Hence, the mechanical properties revealed the optimum toughness as well as flexibility of F5 film 60:40, CH–TP proportions but the film F4 had shown low flexibility and tensile strength.

3.6. Zeta potential and conductivity

Zeta potential is an indicator of the net charge present on the particles or films surface. It is often used in conjunction with conductivity to judge the contribution of charged moieties present in polymeric materials. The data pertaining to zeta potential and conductivity of films are presented in Fig. 5C.

The lowest negative zeta potential and minimum conductivity of F5 film composition technique indicated uniform distribution of interaction density (between $-COO^-$ moieties of TP and $-NH_3^+$ moieties of CH). This could be attributed to optimum interaction between $-COO^-$ groups of galacturonic acid monomer of TP and $-NH_3^+$ groups of CH. Similarly, conductivity was highest for F4 film

that contained 50:50 ratio of CH:TP. It was minimum for F5 films containing 60:40 proportions of CH and TP suggesting least availability of charged functional groups due to optimum interaction between CH and TP during film formation.

It is worthy to note that decrease in magnitude of zeta potential in the films was accompanied with increase in ΔH of first and second endothermic transitions observed in DSC analysis (Table 2). The observations suggested presence of ionized functional groups of CH or TP that contributed to zeta potential to result in depression in endothermic transitions. Thus, minimum negative zeta potential of F5 film seems logical due to availability of least number of ionized groups owing to optimum interaction of $-COO^-$ and $-NH_3^+$ groups.

3.7. Evaluating CH–TP as tablet coating material

The ideal coating material is one that displays the highest binding of coating material (CH–TP) with the tablet surface. Secondly, after drying, the coat of the coated tablet should exhibit negligible stickiness. Improper adhesion of the tablet coatings over the tablet surface may produce a coated surface that can be easily peeled off. Both interfacial interactions and internal stress between the coat and tablet surface dictate the adhesiveness of the coat. Internal stress arises due to shrinkage of the film upon solvent evaporation, thermal stress due to variation in thermal expansion of the tablet surface and film and volumetric stress as the tablet surface swells during storage. Thus, evaluation of adhesive force strength is an indicator of tablet coat behaviour. Hence, an attempt was made to study these two essential properties using a texture analyzer by estimating the adhesive force strength and cohesive force strength of the tablet coating. Adhesive force strength indicated the force required to separate the film coating from the coated tablets. Cohesive force strength revealed stickiness among the coated tablets. The uncoated tablets were observed to exhibit negligible adhesive force strength (Table 2). However, CH–TP coated tablet showed significant difference in adhesive force strength. The results suggested adhesive force strength of CH–TP coated tablets when coated with 60:40::CH:TP composition of coating solution was maximum. This indicated enhanced binding of tablet coat with tablet surface. The reduced adhesive force strength, when tablets coated with 50:50 composition of CH–TP was associated with high magnitude of zeta potential (Fig. 5C) of F4 films (50:50::CH:TP). However, the minimum adhesive force strength of T3 coated tablets batch could be due to reduction in pectin content (30 parts) and increase in CH proportion (70 parts). The positivity induced by CH in a CH:TP::70:30 solution over the positively charge tablet surface generated repulsive forces. This leads to negligible adhesion of coat over tablet surface. Further, no significant difference in adhesive force strength when examined at different contact time was observed. The results of cohesive force strength indicated negligible cohesive strength of T2 (60:40::CH:TP coating solution) batch tablets as compared to T1 and T3. This seems to be due to high water resistant surface provided by F5 (60:40::CH:TP) films (Fig. 2A). Thus, the findings indicated overwhelming influence of composition of CH and TP on the tablet coating behaviour. Further, the results showed enhanced adhesive force strength of T2 batch tablets as compared to Eudragit L-100 (a non-biodegradable, synthetic, polymethacrylate derivative) coated tablets (TE) suggesting high acceptance of this polysaccharide composition as a tablet coating material.

3.8. Surface morphology

SEM investigations on film coat of T3 tablets were conducted to draw conclusion on how the structure of film surface as well as inside of film varied with different pH conditions and method used to prepare it. The SEM images obtained after peeling the film coat exposed to different pH conditions. The unexposed film coat was found to be smooth, uniform and tightly packed irrespective of method used to prepare it (Fig. 6A and B). Fig. 6C–F showed exposure to pH 1.2 buffer and pH 7.4 buffer did not create any damage/structural changes in the tablet coat of batch T3. However, roughness of film coat was observed when tablet coat exposed to pH 6.8 buffer (Fig. 6G and H). Thus, the findings explain high strength of packaging of tablet coat. Further, the use of this coating material could be widely acceptable for the purpose of coating tablet to bad odour and providing smooth texture, flavour to tablets.

3.9. In vitro performance of CH–TP coated tablets

In vitro drug release behaviour from core/coated mesalamine tablets. The results suggested CH–TP does not interfere in the MA release. This is probably due to rolling effect of CH–TP films. When the tablet coat comes in contact with 0.1 N HCl, it starts on rolling. This leads to peeling of coat and exposure of core tablet directly to 0.1 N HCl. Thus, release of MA from coated tablet was similar to core MA tablet.

The comparison of dissolution profiles of uncoated, control (Eudragit coated), T1–T3 batches of tablets suggested no significant effect on MA release. This was clarified from similarity factor ($f_2 = 81.6$) and dissimilarity factor ($f_1 = 2.3$). The values of $f_1 < 15$ and $f_2 > 50$ are indicative of the similarity of dissolution profiles. The results of uncoated, control (Eudragit coated), T1–T3 batches indicated that the batches are similar.

4. Conclusion

Tamarind pectin contains COO^- moieties (due to presence of galactouronic acid) that had interacted with $-NH_3^+$ moieties of CH to form CH–TP films. The presence of $-O^-$ group in CH and/or TP produces H-bonding among themselves or with each other. This interaction density formed by the interaction between CH and TP produces water resistant film surface. The CH–TP admixture was found to provide smooth and uniform texture to the tablets when spray coated. The difference in the composition of CH–TP coat showed significant difference in adhesive force strength. Further, the adhesive force strength of CH–TP coated tablets was found to be better than Eudragit coated tablets. Thus, the results suggested CH–TP admixture could be used as alternative coating material to already used material in both food and pharmaceutical industry.

Acknowledgements

The authors would like to acknowledge the financial assistance provided to Kuldeep Singh (SRF) by Council of Scientific and Industrial Research, New Delhi, India, vide sanction no. 09/140(0154)/2010/EMR-I. We are also thankful to Coordinator (UGC SAP), Dept. of Pharm. Sc. and Drug Res., Punjabi University, Patiala (India) for extending the facility of Texture analyzer.

References

Al-Fatimi, M., Wurster, M., Schröder, G., & Lindequist, U. (2007). Antioxidant, antimicrobial and cytotoxic activities of selected medicinal plants from Yemen. *Journal of Ethnopharmacology*, *111*, 657–666.

Caluwe, E. D., Halamova, K., & Damme, P. V. (2010). *Tamarindus indica* L. – A review of traditional uses, phytochemistry and pharmacology. *Afrika Focus*, *23*, 53–83.

Chen, P., Kuo, T., Kuo, J., Tseng, Y., Wang, D., Lai, J., et al. (2010). Novel chitosan–pectin composite membranes with enhanced strength, hydrophilicity and controllable disintegration. *Carbohydrate Polymers*, *82*, 1236–1242.

Dutta, R. K., & Sahu, S. (2012). Development of diclofenac sodium loaded magnetic nanocarriers of pectin interacted with chitosan for targeted and sustained drug delivery. *Colloids and Surfaces B: Biointerfaces*, *97*, 19–26.

Einhorn-Stoll, U., & Kunzek, H. (2009). Thermoanalytical characterisation of processing-dependent structural changes and state transitions of citrus pectin. *Food Hydrocolloids*, *23*, 40–52.

El-Siddig, K., Gunasena, H. P. M., Prasad, B. A., Pushpakumara, D. K. N. G., Raman, K. V. R., Viyayanand, P., et al. (2006). Properties of species. In J. T. Williams, R. W. Smith, N. Haq, & Z. Dunisger (Eds.), *Tamarindus indica L. fruits for the future. Southampton centre for underutilized crop, RPM print and design* (pp. 13–18). England: W. Sussex.

Goyal, P., Kumar, V., & Sharma, P. (2008). Graft copolymerization of acrylamide on to tamarind kernel powder in the presence of cerric ion. *Journal of Applied Polymer Science*, *108*, 3696–3701.

Goyal, P., Kumar, V., & Sharma, P. (2007). Carboxymethylation of tamarind kernel powder. *Carbohydrate Polymers*, *69*, 251–255.

Grzegorzewski, F., Sascha, R., Kroh, L. W., Geyer, M., & Schluter, O. (2010). Surface morphology and chemical composition of lamb's lettuce (*Valerianella locusta*) after exposure to a low-pressure oxygen plasma. *Food Chemistry*, *122*, 1145–1152.

Hiorth, M., Kjoniksen, A., Knudsen, K. D., Sande, S. A., & Nystrom, B. (2005). Structural and dynamical properties of aqueous mixtures of pectin and chitosan. *European Polymer Journal*, *41*, 1718–1728.

Hiorth, M., Tho, I., & Sande, S. A. (2003). The formation and permeability of drugs across free pectin and chitosan films prepared by a spraying method. *European Journal of Pharmaceutics and Biopharmaceutics*, *56*, 175–182.

Itoh, K., Yahaba, M., Takahanshi, A., Tsuruya, R., Miyazaki, S., Dairaku, M., et al. (2008). In situ gelling xyloglucan/petin formulations for oral sustained drug delivery. *International Journal of Pharmaceutics*, *356*, 95–101.

Jindal, V., Dhingra, D., Sharma, S., Parle, M., & Harna, R. K. (2011). Hypolipidemic and weight reducing activity of the ethanolic extract of *Tamarindus indica* fruit pulp in cafeteria diet and sulpiride-induced obese rats. *Journal of Pharmacology and Pharmacotherapy*, *80*, 80–84.

Jindal, M., Kumar, V., Rana, V., & Tiwary, A. K. (2013a). *Aegle marmelos* fruit pectin for food and pharmaceuticals: Physico-chemical, rheological and functional performance. *Carbohydrate Polymers*, *93*, 386–394.

Jindal, M., Kumar, V., Rana, V., & Tiwary, A. K. (2013b). An insight into the properties of Aegle marmelos pectin–chitosan cross-linked films. *International Journal of Biological Macromolecules*, *52*, 77–84.

Kaur, G., Jain, S., & Tiwary, A. K. (2010). Chitosan-carboxymethyl tamarind kernel powder interpolymer complexation: Investigations for colon drug delivery. *Scientia Pharmaceutica*, *78*, 57–78.

Kaur, G., Mahajan, M., & Bassi, P. (2013). Derivatized polysaccharides: Preparation, characterization, and application as bioadhesive polymer for drug delivery. *International Journal of Polymeric Materials and Polymeric Biomaterials*, *62*, 475–481.

Kaur, H., Yadav, S., Ahuja, M., & Dilbaghi, N. (2012). Synthesis; characterization and evaluation of thiolated tamarind seed polysaccharide as a mucoadhesive polymer. *Carbohydrate Polymers*, *90*, 1543–1549.

Kulkarni, M. G., Thakar M. J., Kulkarni, S. S., Nene, S. N., Thakar, M. J., Gaikwad, B. G. (2001). Process for the recovery of potassium bitartrate and other products from tamarind pulp. US patent no: 5,994,533.

Kumar, C. S., & Bhattacharya, S. (2008). Tamarind seed: Properties. Processing and utilization. *Critical Reviews in Food Science and Nutrition*, *48*, 1–20.

Lim, C. Y., Mat Junit, S., Abdulla, M. A., & Abdul Aziz, A. (2013). In vivo biochemical and GENE expression analyses of the antioxidant activities and hypocholesterolaemic properties of *Tamarindus indica* fruit pulp extract. *PLoS ONE*, *23*, 1–12.

Lootens, D., Capel, F., Durand, D., Nicolai, T., Boulenguer, P., & Langendorff, V. (2003). Influence of pH Ca concentration, temperature and amidation on the gelation of low methoxyl pectin. *Food Hydrocolloids*, *17*, 237–244.

Luppi, B., Bigucci, F., Abruzzo, A., Corace, G., Cerchiara, T., & Zecchi, V. (2010). Freeze-dried chitosan/pectin nasal inserts for antipsychotic drug delivery. *European Journal of Pharmaceutics and Biopharmaceutics*, *75*, 381–387.

Morris, G. A., Foster, T. J., & Harding, S. E. (2000). The effect of degree of esterification on the hydrodynamic properties of citrus pectin. *Food Hydrocolloids*, *14*, 227–235.

Morris, G. A., Kok, M. S., Harding, S. E., & Adams, G. G. (2010). Polysaccharide drug delivery systems based on pectin and chitosan. *Biotechnology and Genetic Engineering Reviews*, *27*, 257–284.

Muzzarelli, C., Stani, V., Gobbi, L., Tosi, G., & Muzzarelli, R. A. A. (2004). Spray drying of solutions containing chitosan together with polyuronans and characterization of the microspheres. *Carbohydrate Polymers*, *57*, 73–82.

Muzzarelli, R. A. A., Boudrant, J., Meyer, D., Mannod, N., DeMarchis, M., & Paoletti, M. G. (2012). Current views on fungal chitin/chitosan, human chitinases, food preservation, glucans, pectins and inulin: A tribute to Henri Braconnot, precursor of the carbohydrate polymers science, on the chitin bicentennial. *Carbohydrate Polymers*, *87*, 995–1012.

Muzzarelli, R. A. A., & Muzzarelli, C. (2005). Chitosan chemistry: Relevance to the biomedical sciences. In T. Heinze (Ed.), *Advances in polymer science* (pp. 151–209). Berlin: Springer Verlag, 186.

Nwodo, U. U., Obiiyeke, G. E., Chigor, V. N., & Okoh, A. I. (2011). Assessment of *Tamarindus indica* extracts for antibacterial activity. *International Journal of Molecular Science*, *12*, 6385–6396.

Oliveira, G. F., Ferrari, P. C., Carvalho, L. Q., & Evangelista, R. C. (2010). Chitosan–pectin multiparticulate systems associated with enteric polymers for colonic drug delivery. *Carbohydrate Polymers*, *82*, 1004–1009.

Prajapati, V. D., Jani, G. K., Moradiya, N. G., & Randeria, N. P. (2013). Pharmaceutical applications of various natural gums, mucilages and their modified forms. *Carbohydrate Polymers*, *92*, 1685–1699.

Puga, A. M., Lima, A. C., Mano, J. F., Concheiro, A., & Alvarez-Lorenzo, C. (2013). Pectin-coated chitosan microgels crosslinked on superhydrophobic surfaces for 5-fluorouracil encapsulation. *Carbohydrate Polymers*, *98*, 331–340.

Rai, P., Tiwary, A. K., & Rana, V. (2012a). Optimization of an aqueous tablet-coating process containing carboxymethylated *Cassia fistula* Gum. *AAPS PharmSciTech*, *13*, 431–440.

Rai, P., Tiwary, A. K., & Rana, V. (2012b). Superior disintegrating properties of calcium cross-linked Cassia fistula gum derivatives for fast dissolving tablets. *Carbohydrate Polymers*, *87*, 1098–1104.

Rana, V., Rai, P., Tiwary, A. K., Singh, R. S., Kennedy, J. F., & Knill, C. J. (2011). Modified gums: Approaches and applications in drug delivery. *Carbohydrate Polymers*, *83*, 1031–1047.

Sato, A. C. K., Oliveira, P. R., & Cunha, R. L. (2008). Rheology of mixed petin solutions. *Food Biophysics*, *3*, 100–109.

Singh, K., Suri, R., Tiwary, A. K., & Rana, V. (2012). Chitosan films: Crosslinking with EDTA modifies physicochemical and mechanical properties. *Journal of Material Science: Material in Medicine*, *23*, 687–695.

Singh, K., Tiwary, A. K., & Rana, V. (2013a). Spray dried chitosan–EDTA superior microparticles as solid substrate for the oral delivery of Amphotericin B. *International Journal of Biological Macromolecules*, *58*, 310–319.

Singh, K., Tiwary, A. K., & Rana, V. (2013b). Ethylenediaminediaceticacid bis (carbido amide chitosan): Synthesis and evaluation as solid carrier to fabricate nanoemulsion. *Carbohydrate Polymers*, *95*, 303–314.

Singh, K., Kumar, A., Langyan, N., & Ahuja, M. (2009). Evaluation of *Mimosa pudica* seed mucilage as sustained-release excipient. *AAPS PharmSciTech*, *10*, 1121–1127.

Souza, A., & Aka, K. J. (2007). Spasmogenic effect of the aqueous extract of *Tamarindus indica* L. (Caesalpiniaceae) on the contractile activity of guinea-pig taenia coli. *African Journal of Traditional Complement Alternative Medicine*, *16*, 261–266.

Tripathi, S., Mehrotra, G. K., & Dutta, P. K. (2010). Preparation and physicochemical evaluation of chitosan/poly(vinyl alcohol)/pectin ternary film for food-packaging applications. *Carbohydrate Polymers*, *79*, 711–716.

Yapo, B. M. (2011). Pectic substances: From simple pectic polysaccharides to complex pectins – A new hypothetical model. *Carbohydrate Polymers*, *86*, 373–385.